Supplementary Information

Characteristics of pH-regulated aggregation-induced enhanced emission (AIEE) and nanostructure orchestrate via self-assembly of naphthalenediimide-tartaric acid bola-amphiphile: Role in cellular uptake

Sopan M. Wagalgave,[a,b] Mahmood D. Aljabri,[c] Keerti Bhamidipati,[b,d] Deepak A. Shejule,[a] Dinesh N. Nadimetla,[d] Mohammad Al Kobaisi,[c] Nagaprasad Puvvada,[b,d] Sidhanath V. Bhosale,[a,b,*] Sheshanath V. Bhosale[e,*]

[a] Polymers and Functional Materials Division CSIR-Indian Institute of Chemical Technology, Hyderabad 500007, Telangana, India.

[b] Academy of Scientific and Innovative Research (AcSIR), Ghaziabad-201002, India.

[c] School of Science, RMIT University, GPO Box 2476, Melbourne, Victoria 3001, Australia.

[d] Applied Biology Division CSIR-Indian Institute of Chemical Technology, Hyderabad 500007, Telangana, India.

[e] School of Chemical Sciences, Goa University, Taleigao Plateau, Goa-403206, India.

Corresponding authors: S.V.B. (CSIR-IICT): bhosale@iict.res.in S.V.B. (G.U.) svbhosale@unigoa.ac.in

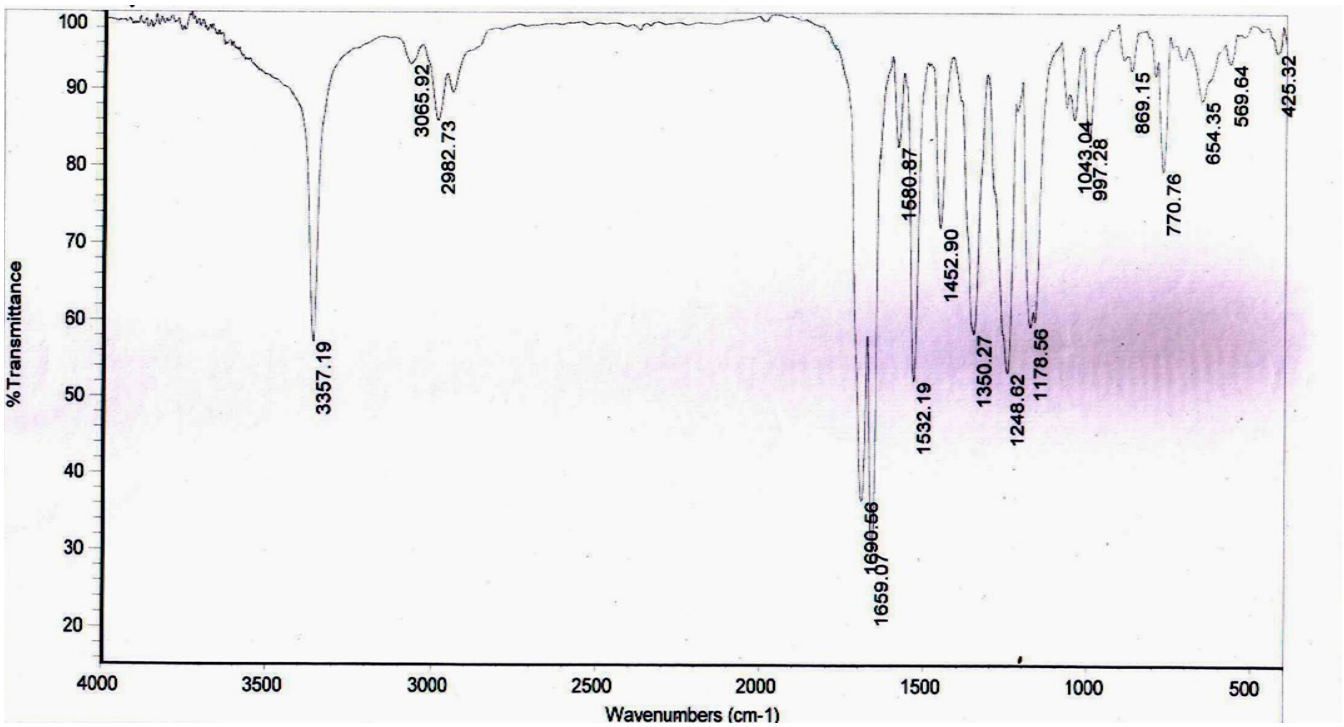

Fig. S1. FT-IR spectra of compound **3**

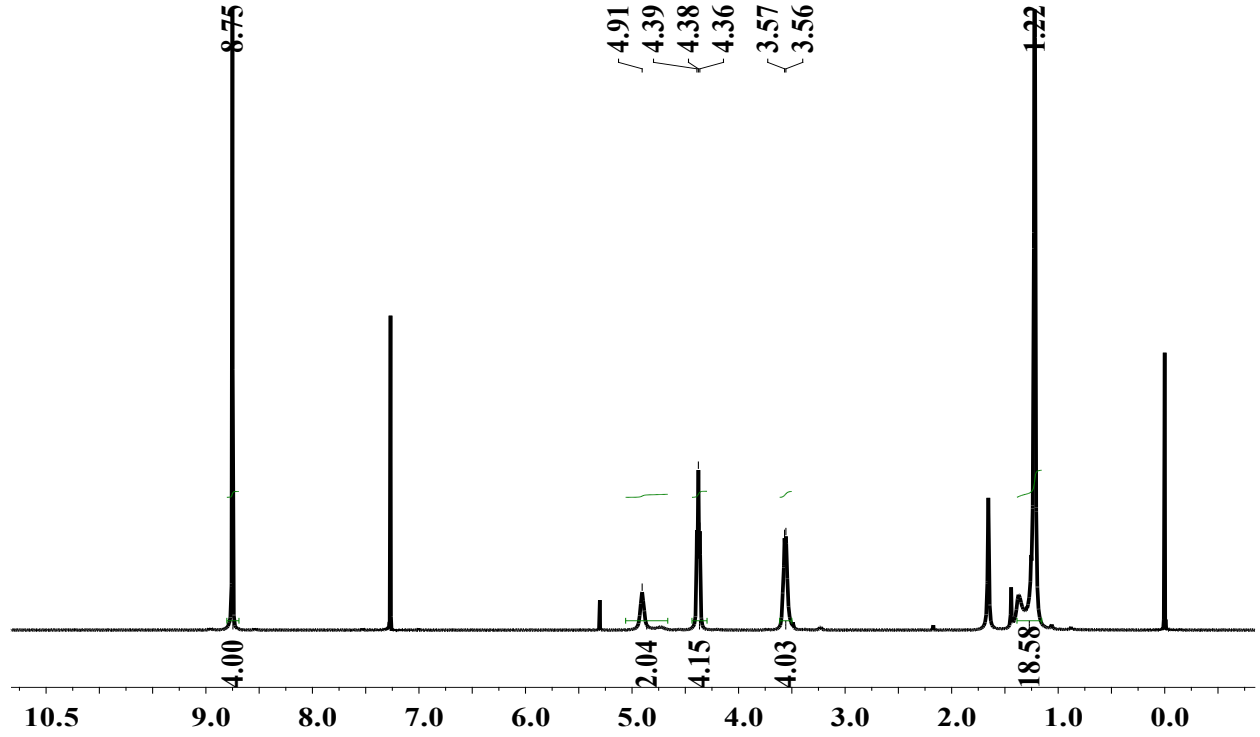

Fig. S2. [1]H NMR spectra of compound **3**

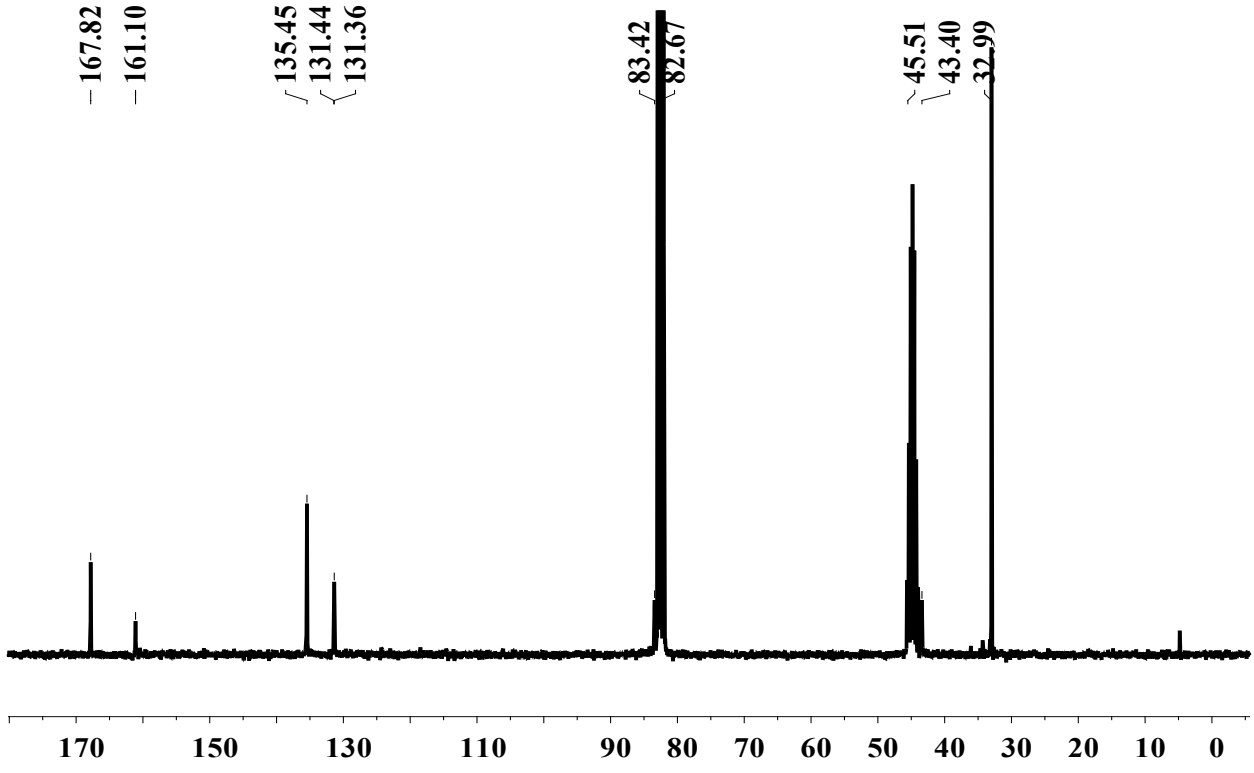

Fig. S3. ^{13}C NMR spectra of compound **3**

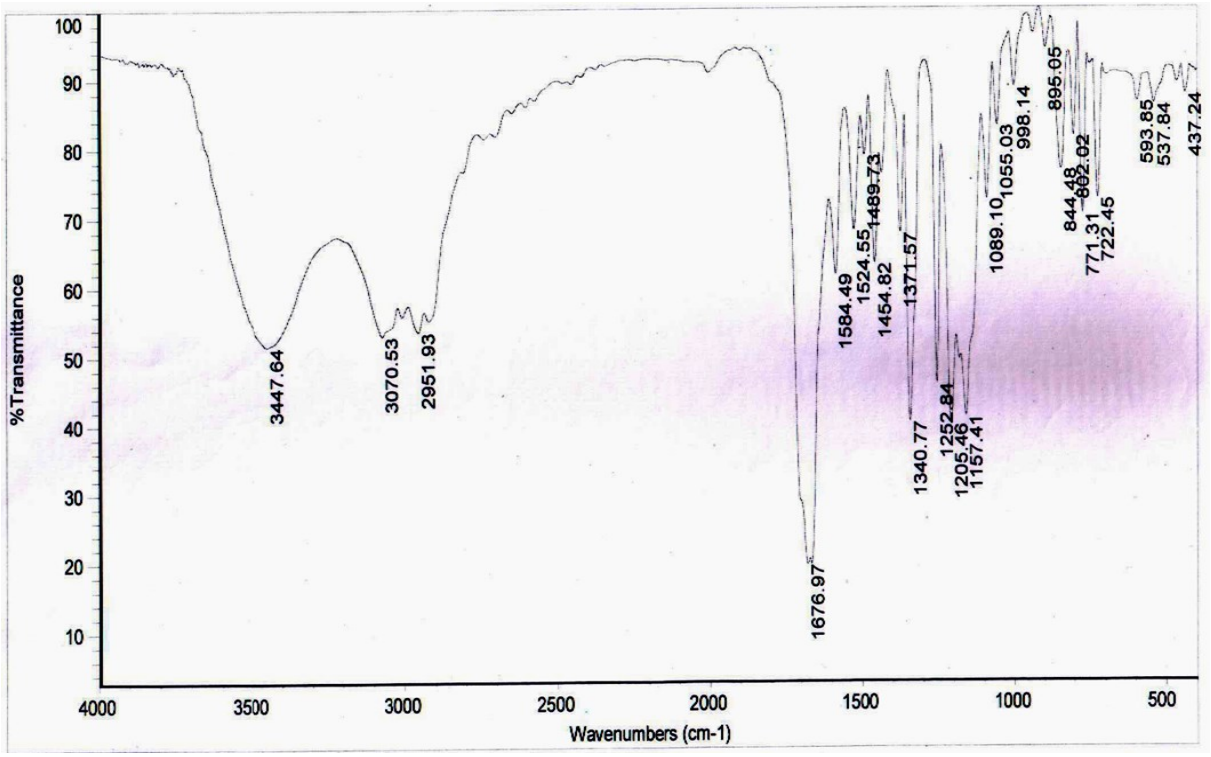

Fig. S4. FT-IR spectra of compound **4**

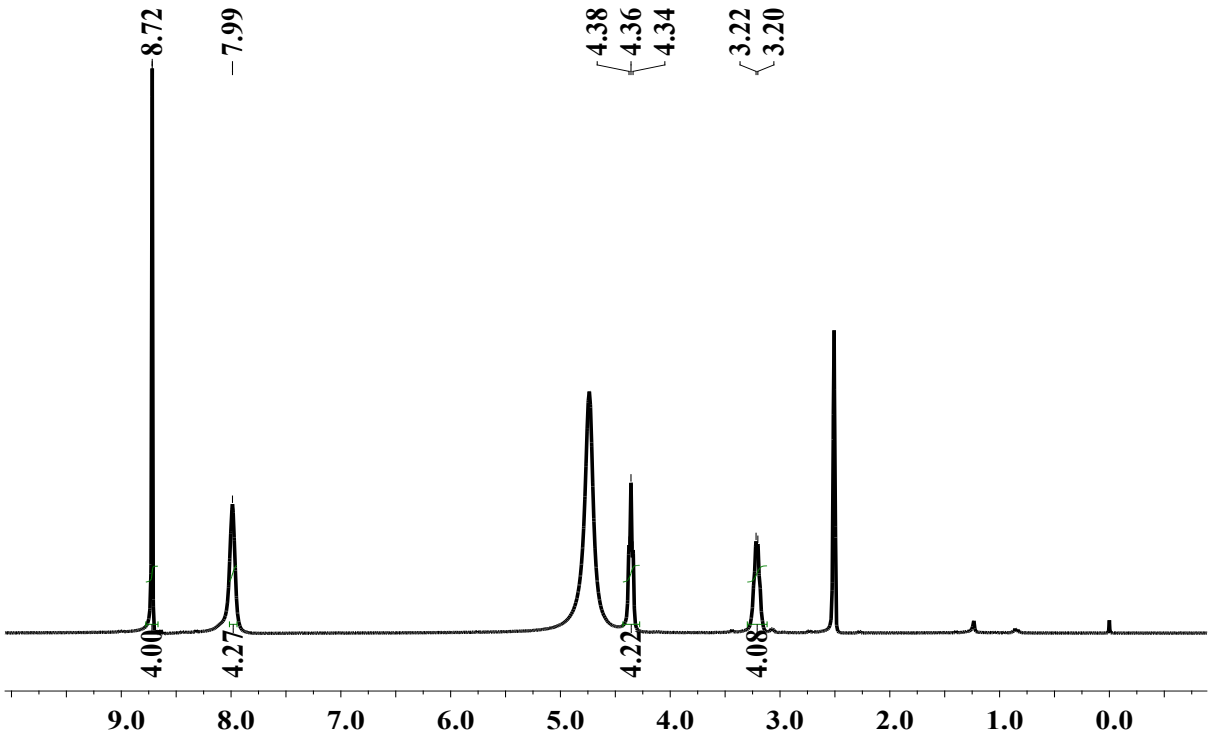

Fig. S5. ^{1}H NMR spectra of compound **4**

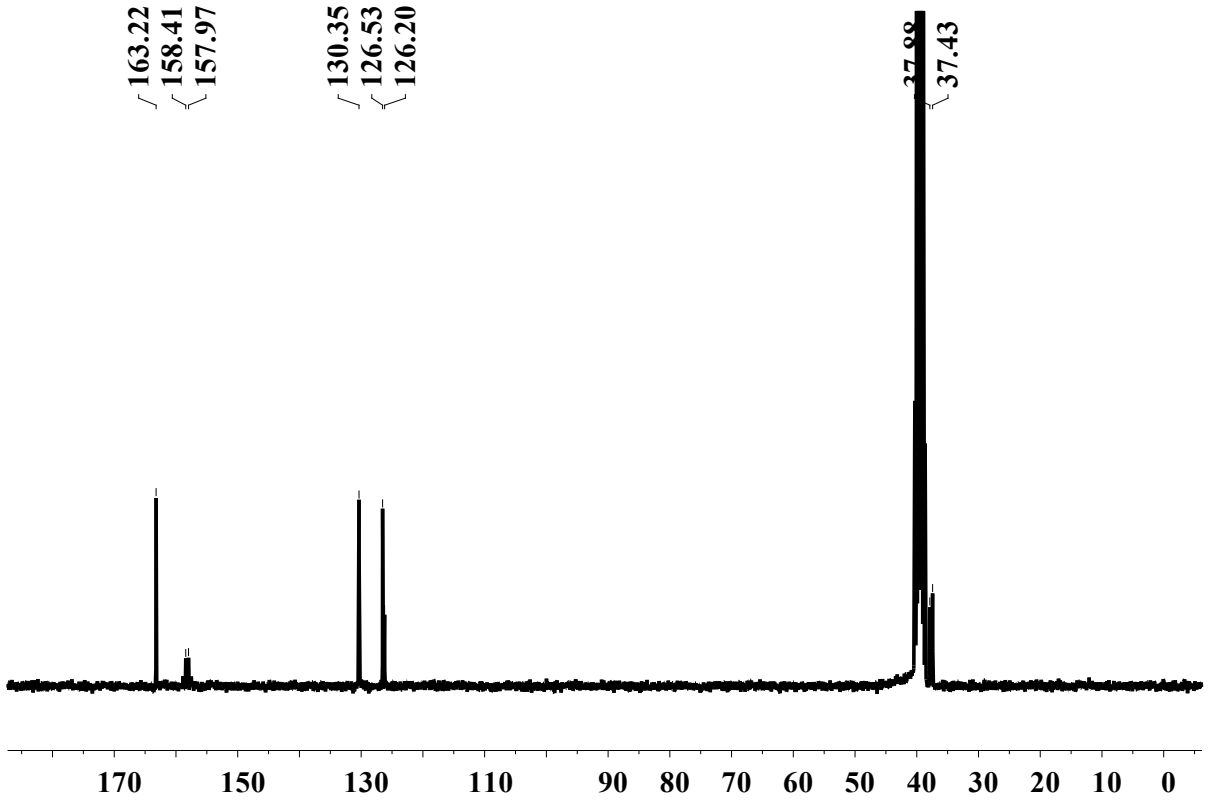

Fi

g. S6. ^{13}C NMR spectra of compound **4**

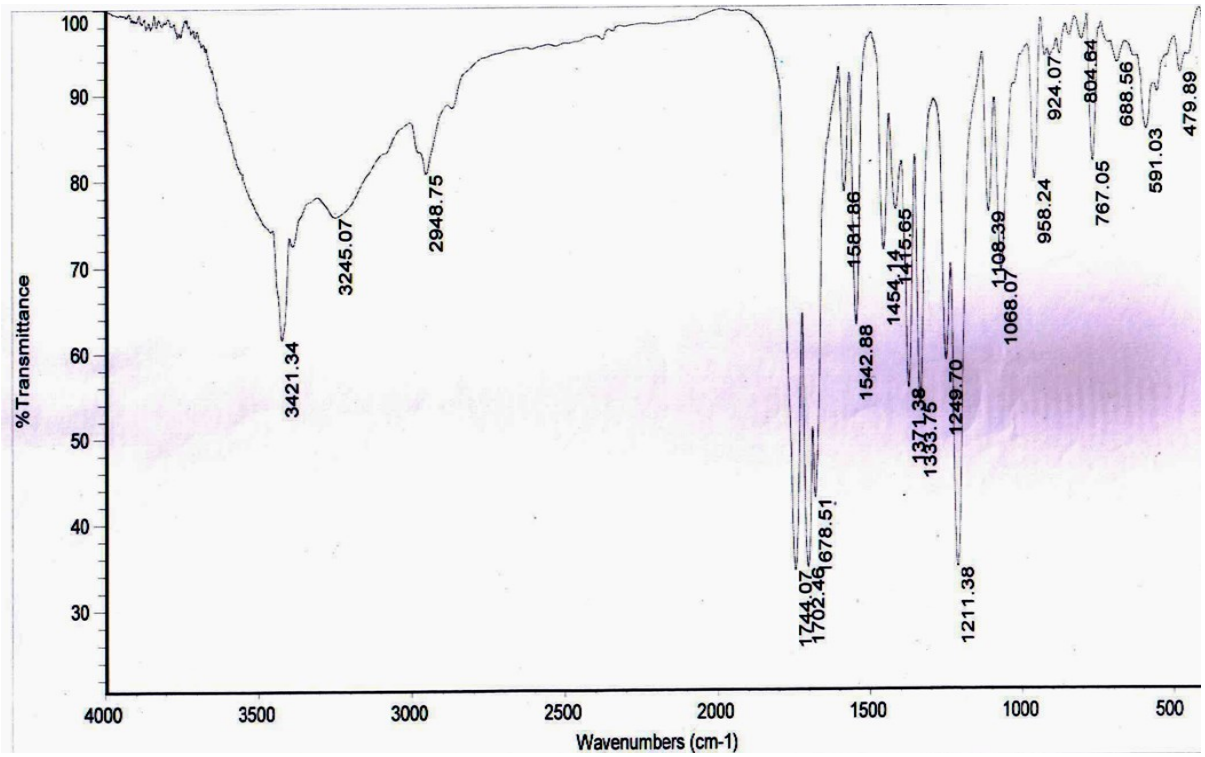

Fig. S7. FT-IR spectra of **NDI-TA**

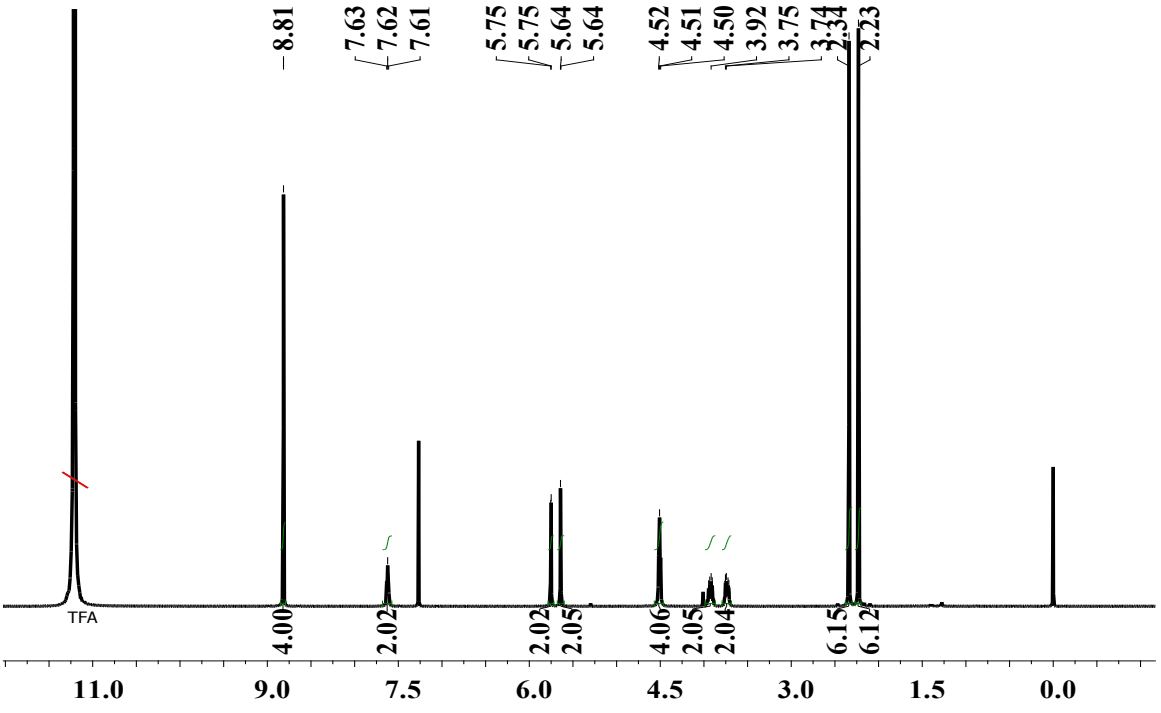

Fig. S8. [1]H NMR of **NDI-TA**

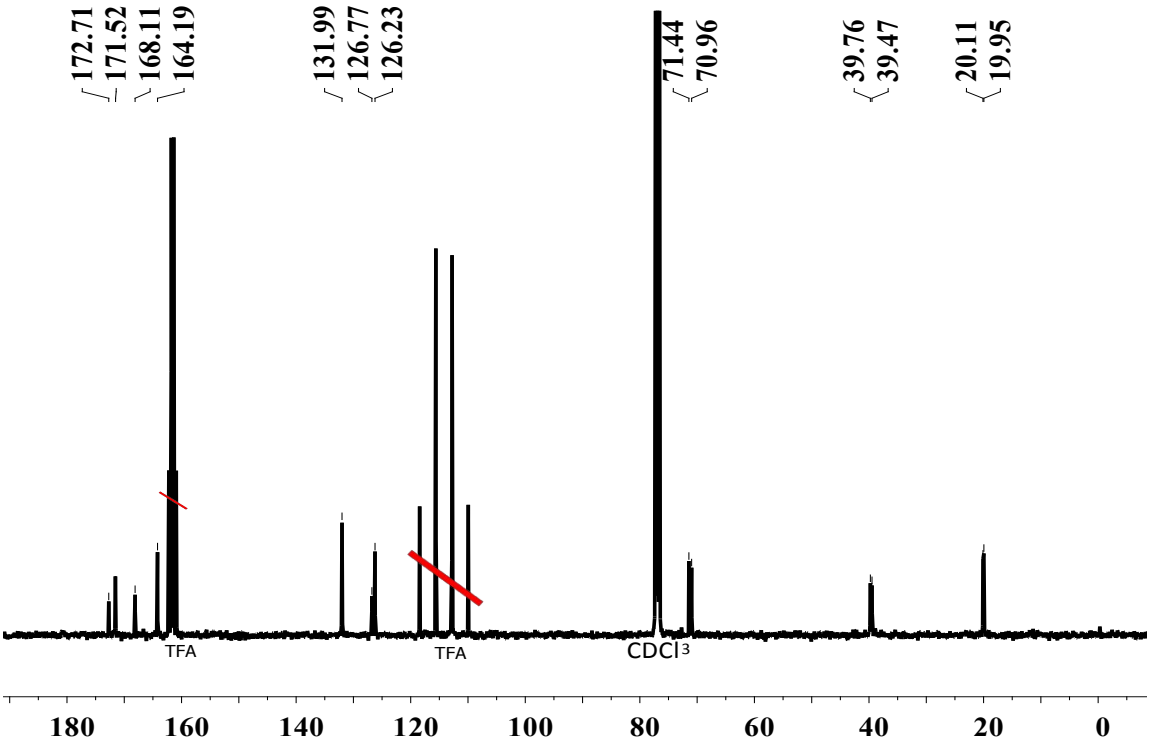

Fig. S9. [13]C NMR spectra of **NDI-TA**

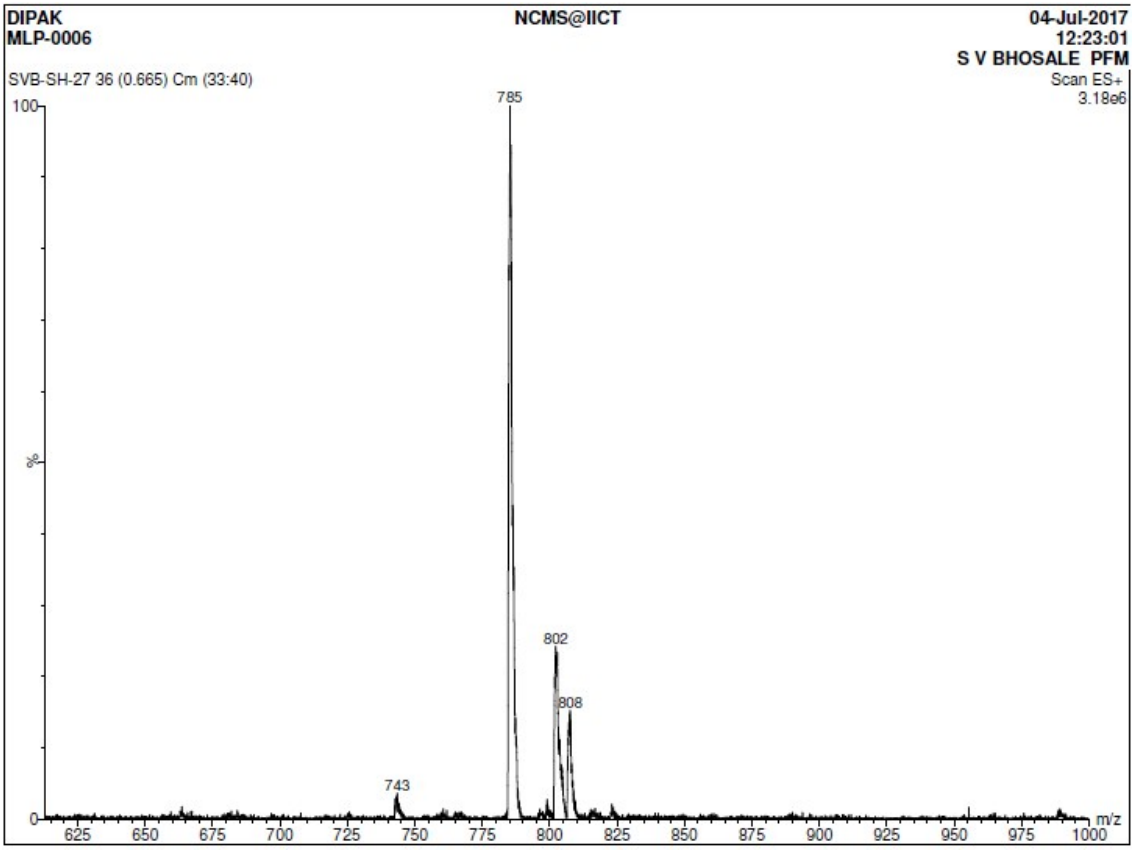

Fig. S10. ESI-MS Spectrum of **NDI-TA**

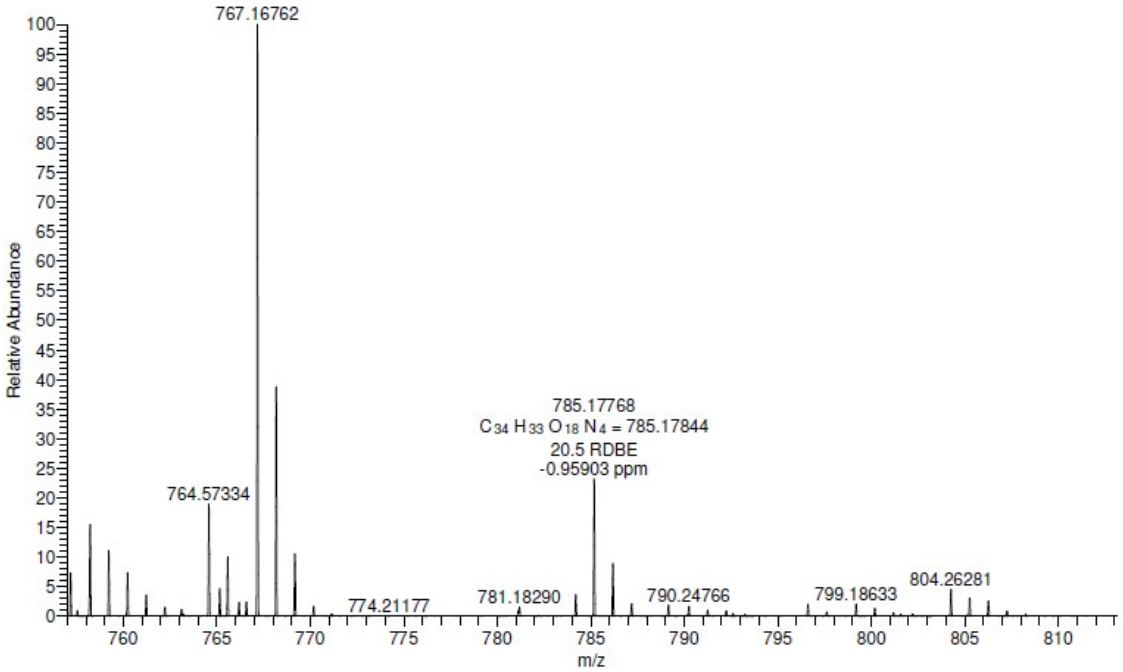

Fig. S11. HRMS Spectrum of **NDI-TA**

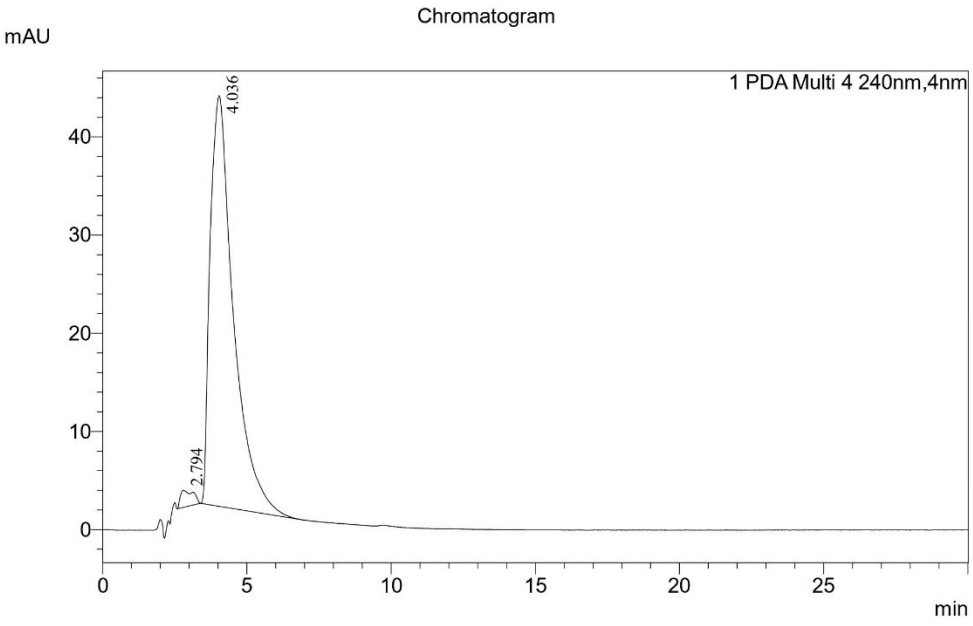

Peak Table

PDA Ch4 240nm

Peak#	Ret. Time	Area	Height	Height%	Area%
1	2.794	52417	1764	4.047	2.189
2	4.036	2341873	41829	95.953	97.811
Total		2394290	43593	100.000	100.000

Fig. S12. HPLC analysis of NDI-TA.

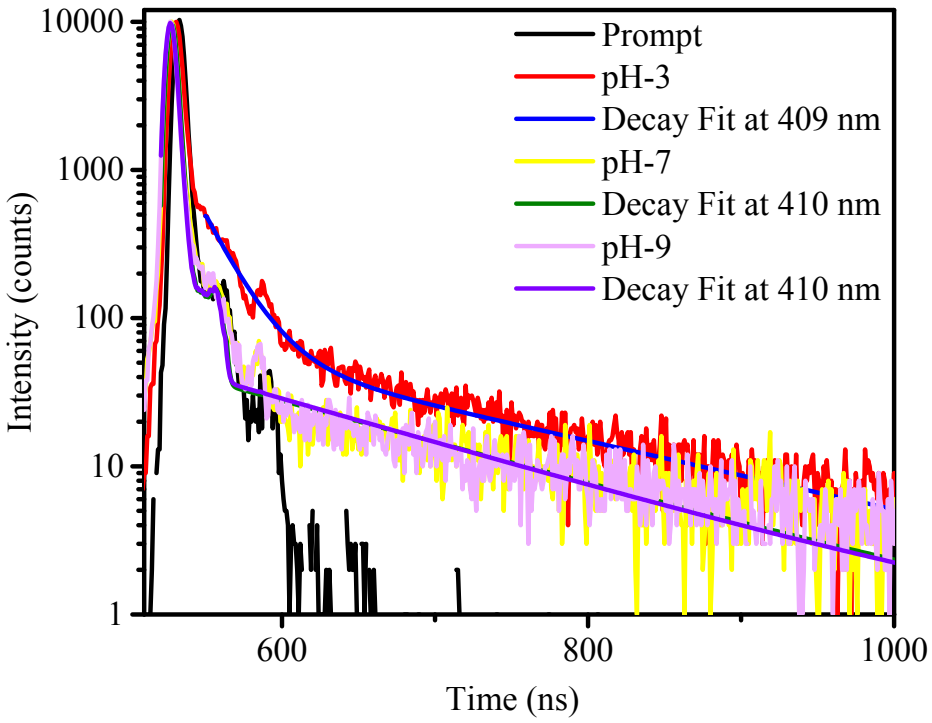

Fig. S13. Flurescence decay of NDI-TA; pH-3, pH-7 and pH-9 (λ_{ex}= 370 nm)

Table S1. Flurescence decay in difference pH solution of NDI-TA.

Sample Code	τ_1 (ns)	Contribution (%)	τ_2 (ns)	Contribution (%)
pH-3	0.569	52.69	5.171	47.31
pH-7	4.305	4.71	0.030	95.29
pH-9	4.063	4.87	0.034	95.13

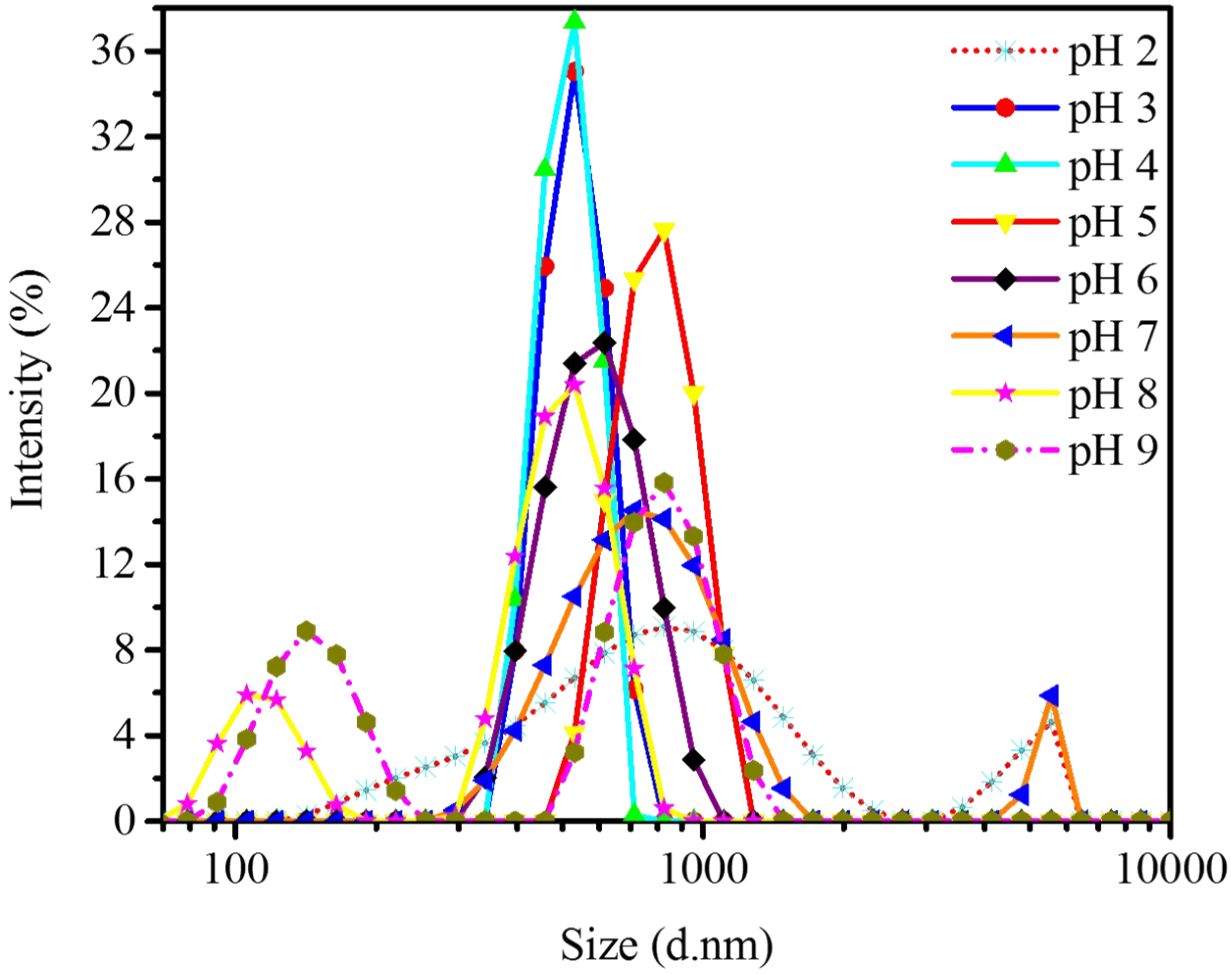

Fig. S14. Dynamic light scattering of NDI-TA at different pH.

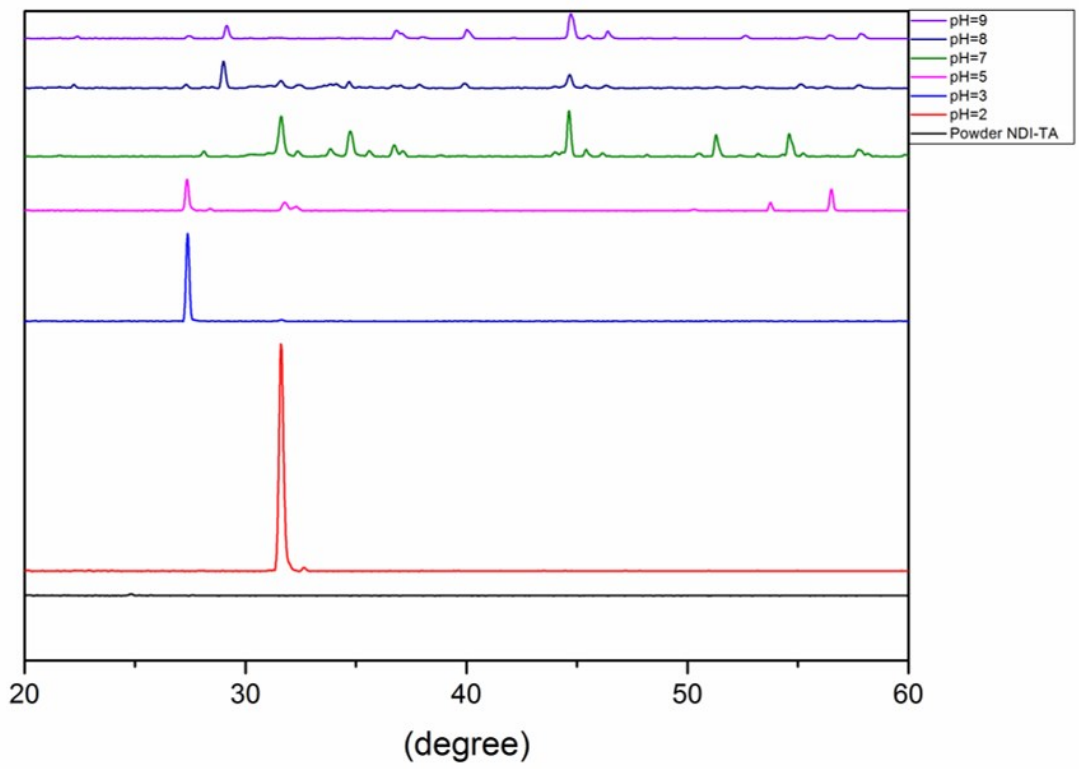

Fig. S15. X-ray powder diffraction (XRD) of pure NDI-TA powder and different pH solutions (2 to 9) which were deposited from the solutions.

Table S2. NDI-TA electronic transitions as calculated in vacuo using TDDFT at B3LYP/6-311+G(d,p) level of theory and Gauss-Sum 3.0 program.

No.	Wavelength (nm)	*f*	Major contributions	Minor contributions
1	393.7	0	H-7→LUMO (95%)	
2	389.0	0.0184	H-4→LUMO (12%), HOMO→LUMO (86%)	
3	388.7	0	H-3→LUMO (12%), H-1→LUMO (87%)	
4	383.0	0.0022	H-5→LUMO (77%), H-4→LUMO (18%)	HOMO→LUMO (4%)
5	382.8	0.3333	H-2→LUMO (93%)	HOMO→LUMO (3%)
6	381.5	0.0011	H-6→LUMO (62%), H-3→LUMO (30%)	H-1→LUMO (6%)
7	377.6	0.0003	H-6→LUMO (34%), H-3→LUMO (57%)	H-1→LUMO (7%)
8	377.3	0.0494	H-5→LUMO (21%), H-4→LUMO (67%)	H-2→LUMO (4%), HOMO→LUMO (8%)
9	376.4	0.0002	H-11→LUMO (95%)	H-7→L+3 (2%)
10	346.4	0	H-16→LUMO (39%), H-12→LUMO (55%)	
11	344.0	0.0257	H-10→LUMO (61%), H-8→LUMO (27%)	H-6→LUMO (2%), H-2→L+2 (5%)
12	329.4	0.0084	H-17→LUMO (58%), H-15→LUMO (24%)	H-19→LUMO (8%), H-7→L+1 (3%)
13	321.4	0	H-9→LUMO (95%)	H-16→LUMO (2%)
14	321.0	0.0012	H-10→LUMO (30%), H-8→LUMO (69%)	
15	313.6	0	H-16→LUMO (53%), H-12→LUMO (37%)	H-20→LUMO (4%), H-9→LUMO (4%)

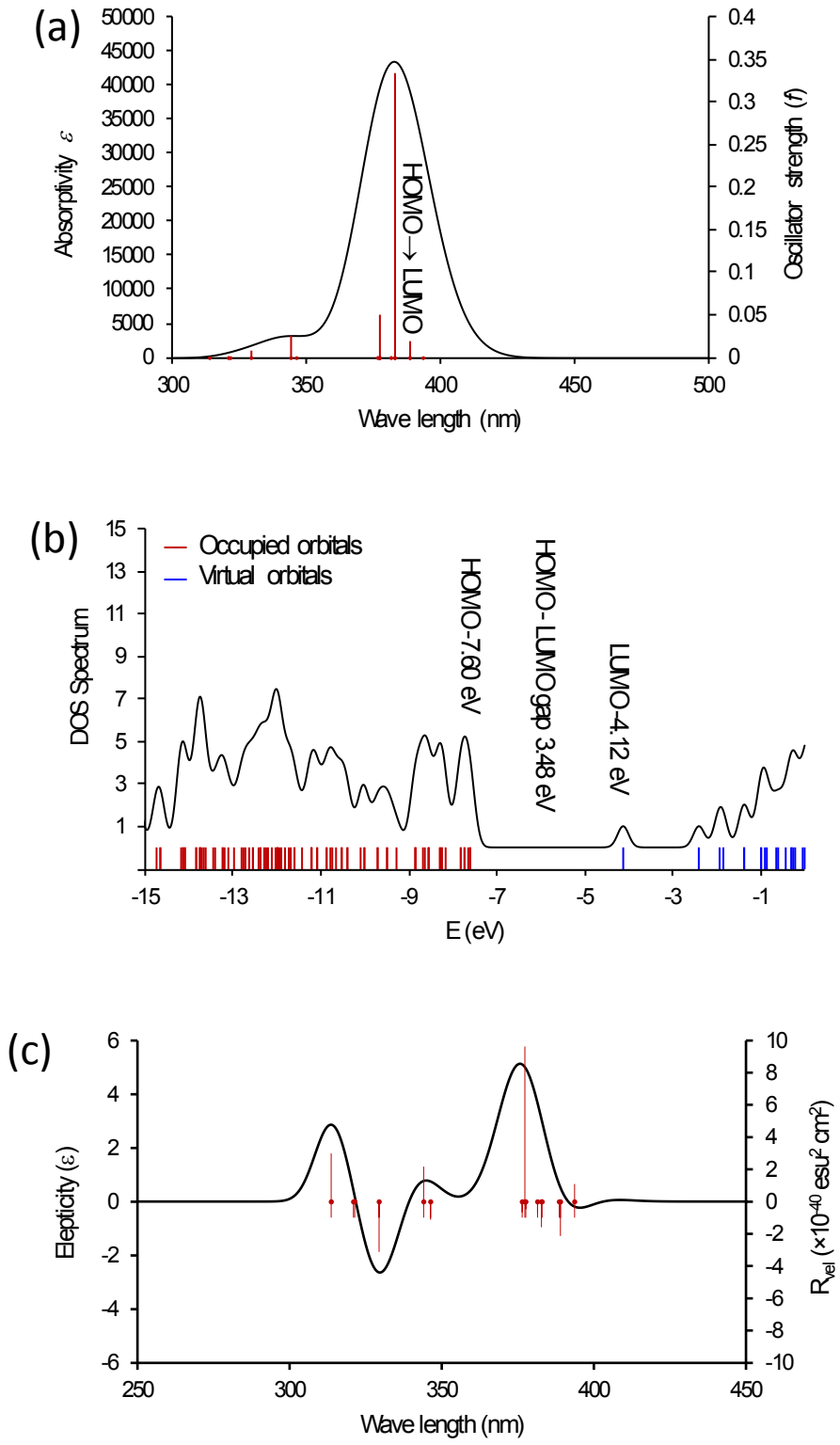

Fig. S16. The UV-vis (a) and DOS (b) spectra simulated using optical transitions of NDI-TA as calculated using TDDFT at B3LYP/6-311+G(d,p) level of theory and Gauss-Sum 3.0 program.